International Journal of Informatics and Communication Technology (IJ-ICT)
Vol. 15, No. 1, March 2026, pp. 405~413
ISSN: 2252-8776, DOI: 10.11591/ijict.v15i1.pp405-413

Detection model for pulmonary tuberculosis and performance evaluation on histogram enhanced augmented X-rays

Abdul Karim Siddiqui[1], Vijay Kumar Garg[2]
[1]School of Computer Science and Application, Lovely Professional University, Phagwara, India
[2]School of Computer Science and Engineering, Lovely Professional University, Phagwara, India

Article Info

Article history:

Received Oct 23, 2024
Revised Sep 28, 2025
Accepted Nov 5, 2025

Keywords:

Deep learning
Intelligent model
Pulmonary TB
TB detection
Tuberculosis

ABSTRACT

Tuberculosis (TB) has remained a big concern for decades. Being contagious millions of lives have been facing life threats, especially in under developing countries who have less resources to neutralize it. The deprived society yields TB infection due to incomplete treatments and the less or no preventive measures. The current time demands an effective effort to eradicate pulmonary TB disease. TB affects lungs in most cases with some other soft organs when not treated properly. Deep learning (DL) has potential to predict and diagnose the severity of pulmonary and extra pulmonary cases. It is a subset of machine learning (ML) that classifies incurable and fatal problems with multi-neural architectures. It helps medical practitioners to identify bacterial infections in the early stage. It has also enabled proper diagnosis and treatment for pulmonary TB. This paper introduces an improved method for detecting and distinguishing between pulmonary TB and normal cases using clinical X-ray images. It uses enhanced radiographs, processed through histogram equalization, and applies them to commonly used classifiers. Two best performing base classifiers were passed into stacked ensemble classifier. By combining multiple models, XGBoost could reduce variance in predictions, leading to higher accuracy. The ensemble classifier showed the best accuracy 99.6% on preprocessed chest X-rays.

Corresponding Author:

Abdul Karim Siddiqui
School of Computer Science and Application, Lovely Professional University
Phagwara, India
Email: abdul.momentum@hotmail.com

1. INTRODUCTION

Tuberculosis (TB) is termed as one of the severe contagious issues worldwide. A person suffering from TB may contain mycobacterium TB bacteria and may transmit the infection during coughing or while talking to a person near them. The droplets that exist in the air medium can be passed even by sneezing. It multiplies when a healthy person comes in close physical contact with a TB-infected person. It hurts one's lungs and is called pulmonary TB. It has remained a global challenge for decades. Developing countries apply the traditional TB diagnostic practices to eradicate it from society. As per WHO data, TB is one of the fatal life-threatening challenges. Mostly, the South Asian countries have high fatality rates. Millions of the young generation are at risk. Regarding Indian subcontinent, the rural Indians need proper attention and care, where effective healthcare setups mandates neutralization of TB. Building on previous work [1] adapted a TB detection module to focus on lung field segmentation and attempted 95.6% accuracy. ML can acquire from unsupervised data. Even when input is unstructured or lacks proper labeling, it predicts more sophistically.

Multi-layer neural network consists of several layers of neurons, serving as a unique model to address various real-world scenarios. It does predictions somehow as human beings.

By up scaling the self-learning feature, DL processes data to bring meaningful results. The connected nodes are referred to as neurons. Filtering and gamma correction were supplied by [2] in the TB model. Abbas *et al.* [3] worked on DeTraC using transfer learning. He used imbalanced datasets. By introducing parametric variations in CNN architecture, he brought detection of PTB-positive cases. Hooda *et al.* [4] used a DL to examine TB in binary classifications and secured 82% accuracy. Schloar [5] presented a CAD system for lung image pattern recognition on CNNs. He got an accuracy of 88%. Meraj *et al.* [6] compared the various classifiers, viz. VGGs, GoogLeNet, and Residual Net50. Yadav *et al.* [7] sketched TB diagnostics on a similar CNN-based transfer learning, getting 94% accuracy. Rahman *et al.* [8] examined nine CNN classifiers for the segmentation process and for the classification. He secured 96% accuracy in his work. Dasanayaka and Dissanayake [9], he used an ensemble model on two base classifiers using TB radiographs. He mentioned an accuracy of 0.971. The investigators [10] used image enhancement techniques and fed the radiographs into the ResNet, and a few other DL models to get higher accuracy that existed 89%. The investigators [11] proposes CNNs to classify obtained clinical images' abnormalities in an ensemble environment. That study [12] used a generalized pre-trained system. They got accuracies of 81.25% with image augmentation and 80% without it simultaneously. Their study incorporated leading state-of-the-art pre-trained deep CNNs for chest radiographs for the classification. It distinguished between normal and PTB-infected cases. Lopes and Valiati [13] used public X-ray labeled datasets. Pre-trained CNNs were used as classifiers and claimed an accuracy of up to 96.1%. Mizan *et al.* [14], DCNNs are highly effective for TB detection from chest X-ray images, with ResNet50 emerging as the most efficient model among those tested. Cao *et al.* [15] emphasized CNNs as highly effective for classifying TB when combined with histogram matching techniques, but their study lacks segmentation. The researchers [16] aimed to compare a custom CNN trained from scratch with several pre-trained CNN models using transfer learning, with a claimed accuracy of 87%. ETDHDNet, proposed by [17], is a DenseNet-based model to integrate extended texture descriptors. The work achieved AUC scores of more than 99 % as claimed. The introduction describes the severity of the problem and worldwide efforts to eradicate pulmonary TB. Related works in this direction using intelligent models are described. Section 2 presents the methodology for the detection system, highlighting preprocessing, data sets description, the proposed system, and experiments. Section 3 explains the results and discussions on various CNN models on TB detection with and without histogram equalization, and a true picture of ensembling base classifiers into a stacked classifier. The conclusion is in section 4 with future work and study to incorporate.

2. RESEARCH METHOD

The overall proposed methodology to detect and classify PTB cases using online and offline Chest X-ray images is described in the methodology section. It uses preprocessing and augmentation of the dataset, Input enhanced by histogram equalization. The ensemble stacked model shows the best of the fused attributes of two different classifiers. Storing the dataset is crucial and is the initial step in prediction model design. It decides the pattern within supervised learning. It also extracts important characteristics during the DL process. Thus, it is of utmost importance to convert image data into a structured and standardized format.

2.1. Datasets description

The M. County CXR set is distinguished by its inclusion of manually segmented lung masks for a subset of its 138 DICOM-format. These images, comprising 80 normal and 58 potentially TB-positive cases, are accompanied by detailed radiology readings in text files. In contrast, the S. Hospital CXR Set, acquired from Shenzhen, China, offers a larger collection of 662 JPEG-format images—326 normal and 336 abnormal—spanning both adult and pediatric cases. The NIAID TB Portals Program stands out as a comprehensive international repository, integrating over 4,200 radiographs (3,500 normal and 700 TB-positive) with multi-domain data linked to individual patients. This includes radiological images, clinical and laboratory reports, genomic data, and socioeconomic and geographic context. Data from TB suspects, including outpatient prescriptions and imaging records from HAHCH in New Delhi, were collected between July 2021 and June 2024, offering a rich resource for holistic TB research and predictive modeling.

2.2. Chest X-ray and feature extraction

The gained chest X-ray images exhibit variations in size and may be either color-grayscale or RGB due to availability from the diverse sources. To guarantee uniformity, all acquired raw data were converted to grayscale. The connected layers that compose CNN architecture insert consistent image dimensions. Preprocessing of all clinical images serves the purpose of enhancing data quality by modifying undesired

distortions and accenting relevant features for subsequent processing and analysis. The ROI, denoting the area of interest, in proposed case-the cavities on the lung surface, is well recognized by the segmentation. This is important step to admit subsequent feature extraction focuses on relevant regions of interest. These features include shape, intensity, texture, and statistical measures.

2.3. Image preprocessing

Preprocessing is the initial step towards data preparation [18]. Before the insertion of the input image into the proposed AI model, datasets are cleaned through various preprocessing techniques. In the proposed work, both online and offline X-ray images had different impurity issues. The online image datasets had size variability with differing image types and colour issues. Similarly, the off-line chest X-ray images had problems like image inversion, rotation, grayscale and coloured images, flipping issue, uncropped images, etc. All these types of odd points were removed using the process of cropping, flipping, resizing, grayscaling, rotation, and type conversion. Although the major X-rays contained one colour channel, some of them had three colour channels. To hide the effect of blue colour, such images were converted from RGB to grayscale. The PNG format was applied to dimensions of 250 X 250 X 3 resolution. Figure 1 contains TB infected areas over lungs. Figure 1(a) is showing infection on the right upper lobe, Figure 1(b) on lymph node, Figure 1(c) on left upper lobe and Figure 1(d) as air space opacities.

Figure 1. Infected area of TB on lungs: (a) coalescing air space opacity on the right upper lobe, (b) enlarged hilar and mediastinal lymph nodes, (c) Thick-walled cavitary lesion in the left upper lobe, and (d) bilateral apical thick-walled cavities multifocal satellite air space opacities

2.4. Augmentation and datsets partion

Image augmentation is resolute step in computer vision and in DL-based classifications. It enriches insourced clinical images by first removing unnecessary details [19]. It should be applied during training only, not during inference as shown in Figure 2. Training datasets are changed into normalized sizes to avoid over-fitting.

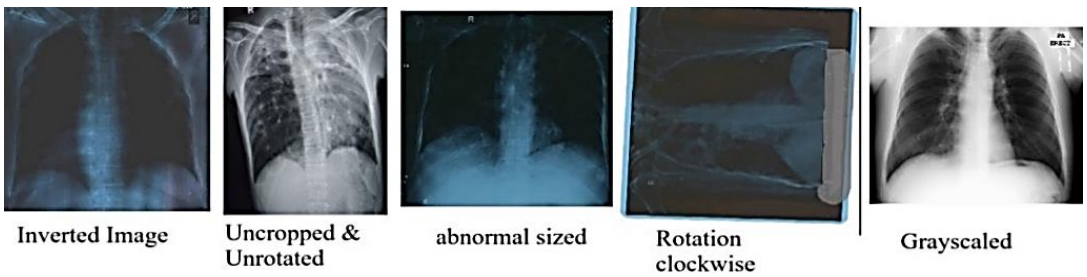

Figure 2. Uncleansed X-ray images

Augmentation is used alongside dataset partitioning with the total image collection divided into 70% for training, 15% for validation, and 15% for testing. A total of 6221 chest X-ray images containing both normal and pulmonary TB cases were collected, with 4355 allocated for training, 933 for validation, and testing, respectively as shown in Table 1. Histogram Equalization is basically a redistribution of pixel intensities so that they become more uniformly distributed across the entire available intensity range. This transformation ensures that the output histogram is approximately uniform [20].

Table 1. Image datasets in the proposed work

Datasets	NORML				PTB			
	Train	Validation	Test	Total	Train	Validation	Test	Total
M. County	56	12	12	80	41	8	9	58
S. Hospital	227	49	49	325	235	51	50	336
NIAD	1674	358	358	2390	490	105	105	700
Belarus	0		0	0	700	150	150	1000
HAHC Hospital	222	48	48	318	710	152	152	1014
TOTAL	2179	467	467	3113	2176	466	466	3108

2.5. Proposed method

Ten different DCNNs are studied so that the outcomes will have atributed X-rays' abnormality detections and thus the initial TB screening and related prediction can be achieved. On the basis of collected Chest radiographs, all state-of-the-art classifiers were trained on the given Training datasets (70% of the total online and real image datasets). On fine-tuning of hyper-parameters, 15% validation datasets were fed into the pre-trained model. The remaining 15% of the untouched datasets were tested on a pre-trained model using transfer learning. On comparing the performance of all the classifiers, the two best-performing base classifiers (ResNet50 and DenseNet169) were passed into a stacked ensemble classifier. Features are extracted from these models' intermediate layers. These extracted features are then concatenated into a single feature vector, which serves as the input for the meta-learner. The XGBoost model is trained to make the final binary classification prediction (PTB-positive or PTB-negative). As shown in Figure 3. This method brings the powerful feature extraction abilities of the CNNs while using XGBoost to learn how to best combine their (pre-trained base classifiers) predictions [21].

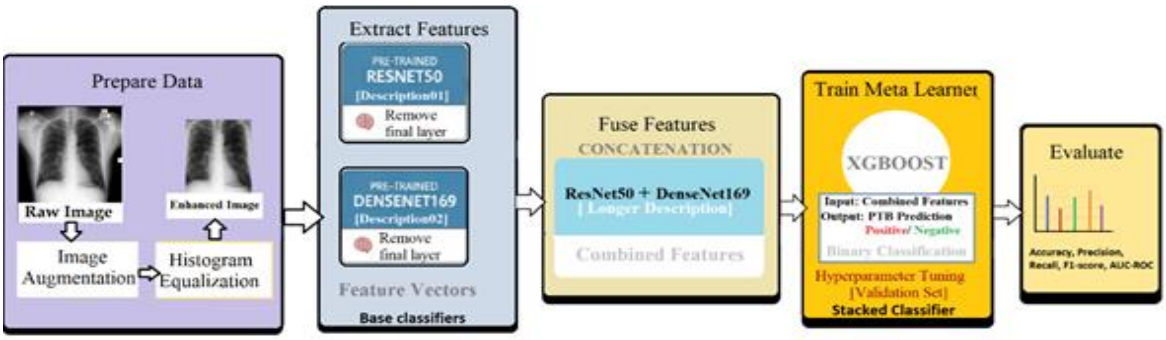

Figure 3. Methodology for the proposed system

2.6. Experiments

Transfer learning supports models to power previously acquired learnings from one task and apply them to a similar task. This approach constitutes a pre-trained model, which has already been trained on a large dataset comprising 4355 images of both normal and PTB cases in the proposed work. By doing so, it considerably reduces training time and computational requirements for new model running while enhancing model accuracy and mitigating the possible issue of overfitting. In CNN-based architecture, TL proves helpful when dealing with small image datasets, eliminating the necessity for extensive data collection and minimizing the training time. In the shared architecture, intermediate weights remain non-trainable, while final layer weights undergo training, with the Sigmoid activation function in the final layer. HE-enhanced images were partitioned into training, validation, and testing sets. For training, 70% of the total images, and 30% for validation and testing were kept respectively. Sklearn.model_selection import train_test_split was set with a random state of 22 for reproducibility. The system also incorporates the Adam optimizer alongside Binary Cross-Entropy as the loss function. The process was executed on the Google Colab using TensorFlow using Python 3.7.10. The training procedure was fine-tuned keeping batch size of 64 and a default threshold of 0.5. To prevent overfitting, epochs were reduced from 15 to 5, ensuring optimal generalization and alignment between training, validation, and testing performance.

3. RESULTS AND DISCUSSION

AI based detection model needs to be verified on different assessment parameters, especially medical diagnostic systems are validated on the following evaluation metrics: 1. Sensitivity 2. Precision 3. Specificity 4. Accuracy 5. F1 score and 6. ROC.

3.1. Performance of CNNs on X-ray dataset without HE

Table 2 is shown to compare the performance of state-of-the-art CNNs for binary classification without using histogram equalization. This comparison is made on preprocessed image inputs collected from five repositories, viz. M. County, S. Hospital [22], NIAD [23], Belarus dataset [24] and images collected during 36 months from the HAHC hospital.

Table 2. Performance matrix of classifiers – Without HE

Model	Resnet50	Resnet 101	Resnet 152	Inception V3	VGG 16	VGG 19	Densenet 121	DenseNet 169	Densenet 201	Mobilenet
Accuracy	99.1	98.4	98.8	94.7	97.8	98	98	98	98.6	98
Sensitivity	99.1	98.5	98.9	93.3	97.9	96.9	98.2	96.6	98.4	98.3
Specificity	99.1	98.3	98.8	97	97.7	99	97.2	99.2	98.3	97.5
Precision	99.1	98.2	98.9	97.3	97.5	98.9	97.3	98.8	98.2	97.4
F1-score	99.1	98.5	98.8	96	97.7	97.9	98	97	98.4	98

The performance is measured on six parameters, basic criteria to check the quality of any medical diagnostic system. It is found that both ResNet50 and ResNet152 outperform the rest of the CNNs without the use of the histogram algorithm. ResNet50 allows gradients to flow through the network more easily, whereas DenseNet201 is intensive due to computationally denser connections. Also, ResNet50 exemplifies the transfer learning here. Other classifiers have shown impressions such as ResNet101, DenseNet201, DenseNet169, and DenseNet121. Figure 4, when evaluating the processed chest X-rays in neural networks without histogram equalization, ResNet50 and ResNet152 have overlapping ROC curves, and both have outstanding ROC, followed by ResNet101. DenseNet also has a better ROC than other classifiers. Here, deeper networks need not perform better results; instead, Resnet50 shows an effective example for transfer learning. A confusion matrix is important for summarization of the performance of a proposed system on 467 normal and 466 PTB test radiographs in Figure 5. Figure 5(a) shows confusion marix for ResNet50 and Figure 5(b) for ResNet152 without histogram equalization.

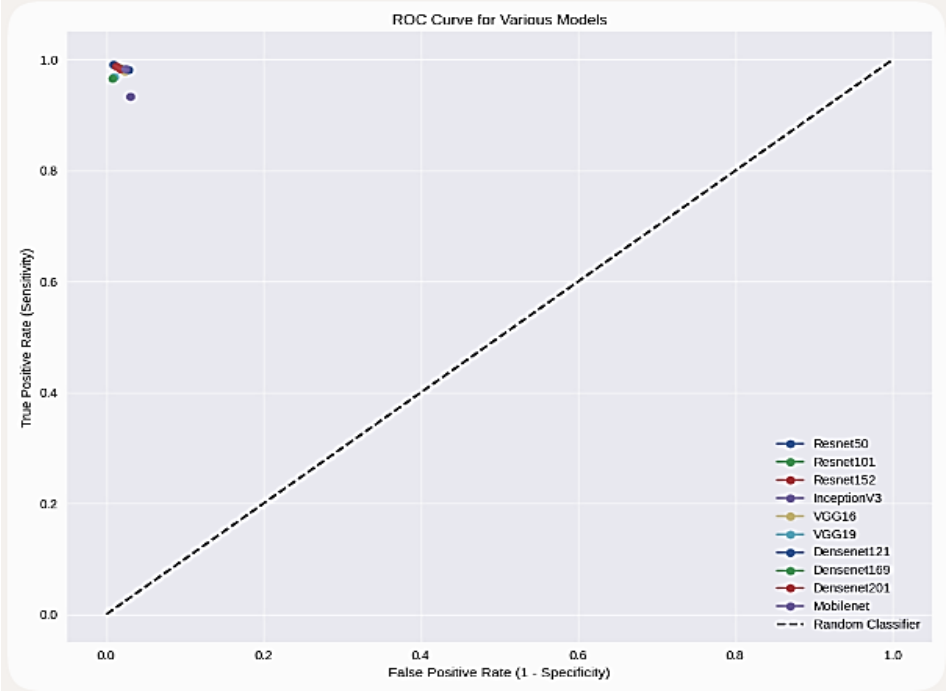

Figure 4. ROC – Various classifiers without HE

ResNet50	Predicted TB	Predicted Normal
Actual TB	TP = 462	FN = 4
Actual Normal	FP = 4	TN = 463

(a)

ResNet152	Predicted TB	Predicted Normal
Actual TB	TP = 461	FN = 5
Actual Normal	FP = 5	TN = 462

(b)

Figure 5. Confusion matrix- without HE (a) Resnet50 and (b) Resnet152

3.2. Performance of classifiers with HE

Table 3 is shown to compare the same sets of data input explained in section 3.1. The performance of all 10 binary classifiers is evaluated on five evaluation matrices and ROC curves on applying HE. It is found that both ResNet50 and DenseNet169 have outmatched the rest of the CNNs by enhancing images with contrast enhancement. ResNet50 allows gradients to flow through the network more easily, whereas DenseNet169 is intensive due to computationally denser connections. Effective sensitivity in DenseNet169 compared to ResNet50 shows improved quality of identifying true positives. Also, ResNet50 exemplifies the transfer learning here. Other classifiers have shown an impression, such as ResNet152, ResNet101, and DenseNet121. ResNe50 has a significant ROC, as in the above case of sensitivity of the model without HE, ResNet152 and 101 also have fewer false negatives, making them a more reliable model for detection. VGG16 and DenseNet201 overlap in the ROC Curve presented in Figure 6.

Table 3. Performance matrix of classifiers – with HE

Model	Resnet50	Resnet 101	Resnet 152	Inception V3	VGG 16	VGG 19	Densenet 121	DenseNet 169	Densenet 201	Mobilenet
Accuracy	**99.36**	99	99.1	95	98.3	98	99	**99.25**	98.6	96.5
Sensitivity	**99.36**	99.1	99.14	95.6	98.4	98.96	98.6	**99.36**	98.4	96.2
Specificity	**99.36**	99	98.8	94.8	98.23	97.1	99.6	**99.14**	98.7	97.1
Precision	**99.36**	98.6	98.7	94.51	98.1	96.95	99	**99.14**	98.61	96.6
F1-score	**99.36**	99	98.9	94.83	98.2	97.5	99.13	**99.2**	98.5	96.5

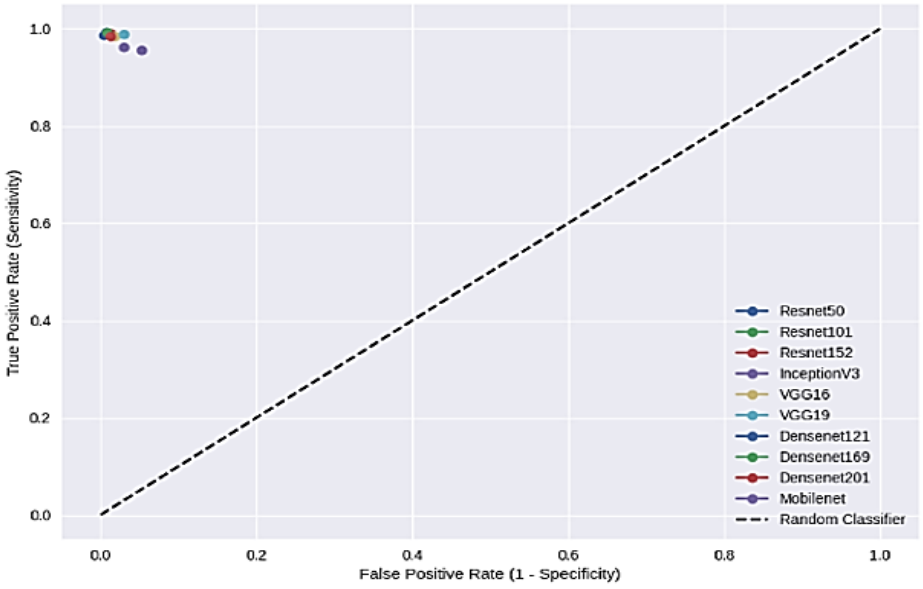

Figure 6. ROC – Various classifiers with HE

Figure 6 presents ROC on different classifiers using HE enhanced X rays. Figure 7 depicts confusion matrix on two best performing classifiers. Binary classifier ResNet50 returned 3 out of 466 TB test radiographs misclassified as normal as in Figure 7(a). 3 out of 467 normal chest test radiographs were misclassified as TB X-ray. In the evaluation of DenseNet169, only 3 out of 466 TB test graphs were misclassified as normal as in Figure 7(b). 4 out of 467 normal CXR test graphs were miscounted as TB images [25].

	Predicted TB	Predicted Normal
Actual TB	TP = 463	FN = 3
Actual Normal	FP = 3	TN = 464

(a)

	Predicted TB	Predicted Normal
Actual TB	TP = 463	FN = 3
Actual Normal	FP = 4	TN = 463

(b)

Figure 7. Confusion matrix- with HE (a) DenseNet169 and (b) Resnet50

3.3. Performance matrics of ensemble stacked classifier

The XGBoost model learnt the optimal way to combine the features from both ResNet50 and DenseNet169 to get the best performance by each ResNet50 and DenseNet169 separately on the given test datasets. Calculating the final model's performance using binary classification, such as accuracy, precision, recall, F1-score, and AUC-ROC on the same test datasets, viz. 467 normal and 466 PTB positive images, the following figures came out. Figure 8 presents to view the confusion matrix for TP, TN, FP, and FN. It shows the outperforming classifiers, viz. DenseNet169 and ResNet50. The combined features revealed from the two base classifiers, the test datasets brought the best performing binary classifier from the XGBoost stacked classifier, as 2 out of 466 TB test radiographs misclassified as normal, 2 out of 467 normal chest test radiographs were misclassified as TB X-ray. It got the best ever accuracy of 99.57%. By evaluating classification performance using histogram matching across 10 deep CNN models, our approach resulted in a more reliable and efficient system, achieving a classification accuracy of 99.57 percent as shown in Table 4.

	Predicted TB	Predicted Normal
Actual TB	TP = 464	FN = 2
Actual Normal	FP = 2	TN = 465

Figure 8. Confusion matrix- ensemble classifier

Table 4. Performance matrix of base classifiers and stacked classifier

Classifier model	Base classifier-1 Resnet50 (without HE)	Base classifier-2 Resnet 152 (without HE)	Base classifier-1 Resnet 50 (with HE)	Base classifier-2 DenseNet 169 (with HE)	Ensemble classifier XGBoost (with HE)
Accuracy	99.1	98.8	99.36	99.25	99.57
Sensitivity	99.1	98.9	99.36	99.36	99.57
Specificity	99.1	98.8	99.36	99.14	99.57
Precision	99.1	98.9	99.36	99.14	99.57
F1-score	99.1	98.8	99.36	99.2	99.57

4. CONCLUSION

The classification results for the pulmonary TB prediction model reveal an exceptionally high level of diagnostic accuracy. Out of all cases evaluated, 464 were correctly identified as TB (True Positives), while only 2 cases were missed (False Negatives), indicating a very low rate of under diagnosis. Similarly, among the normal cases, 465 were accurately classified as non-TB (True Negatives), with just 2 instances misclassified as TB (False Positives). This near-perfect balance between sensitivity and specificity underscores the model's robustness and reliability. The minimal misclassification suggests that the system is highly effective in distinguishing between TB and normal cases, making it suitable for clinical deployment or integration into automated screening workflows. The consistent performance of the ensemble Meta learner across large and varied datasets highlights the robustness and generalizability of our proposed approach.

FUNDING INFORMATION

Authors state no funding involved.

AUTHOR CONTRIBUTIONS STATEMENT

This journal uses the Contributor Roles Taxonomy (CRediT) to recognize individual author contributions, reduce authorship disputes, and facilitate collaboration.

Name of Author	C	M	So	Va	Fo	I	R	D	O	E	Vi	Su	P	Fu
Abdul Karim Siddiqui	✓	✓	✓	✓	✓	✓	✓	✓	✓	✓	✓		✓	
Vijay Kumar Garg	✓						✓	✓		✓		✓	✓	

C : **C**onceptualization
M : **M**ethodology
So : **So**ftware
Va : **Va**lidation
Fo : **Fo**rmal analysis
I : **I**nvestigation
R : **R**esources
D : **D**ata Curation
O : Writing - **O**riginal Draft
E : Writing - Review & **E**diting
Vi : **Vi**sualization
Su : **Su**pervision
P : **P**roject administration
Fu : **Fu**nding acquisition

CONFLICT OF INTEREST STATEMENT

Authors state no conflict of interest.

DATA AVAILABILITY

The data that support the findings of this study are available on request from the corresponding author, [Siddiqui, AK]. The data, which contain information that could compromise the privacy of research participants, are not publicly available due to certain restrictions.

REFERENCES

[1] S. Vajda *et al.*, "Feature selection for automatic tuberculosis screening in frontal chest radiographs," *Journal of Medical Systems*, vol. 42, no. 8, Jun. 2018, doi: 10.1007/s10916-018-0991-9.

[2] P. Chhikara, P. Singh, P. Gupta, and T. Bhatia, "Deep convolutional neural network with transfer learning for detecting pneumonia on chest x-rays," in *Advances in Bioinformatics, Multimedia, and Electronics Circuits and Signals*, Springer Singapore, 2019, pp. 155–168.

[3] A. Abbas, M. M. Abdelsamea, and M. M. Gaber, "DeTrac: transfer learning of class decomposed medical images in convolutional neural networks," *IEEE Access*, vol. 8, pp. 74901–74913, 2020, doi: 10.1109/access.2020.2989273.

[4] R. Hooda, S. Sofat, S. Kaur, A. Mittal, and F. Meriaudeau, "Deep-learning: A potential method for tuberculosis detection using chest radiography," in *2017 IEEE International Conference on Signal and Image Processing Applications (ICSIPA)*, Sep. 2017, pp. 497–502, doi: 10.1109/icsipa.2017.8120663.

[5] L. G. C. Evalgelista and E. B. Guedes, "Computer-aided tuberculosis detection from chest x-ray images with convolutional neural networks," Oct. 2018, doi: 10.5753/eniac.2018.4444.

[6] S. S. Meraj, R. Yaakob, A. Azman, S. N. M. Rum, A. S. A. Nazri, and N. F. Zakaria, "Detection of pulmonary tuberculosis manifestation in chest X-Rays using different convolutional neural network (CNN) models," *International Journal of Engineering and Advanced Technology*, vol. 9, no. 1, pp. 2270–2275, Oct. 2019, doi: 10.35940/ijeat.a2632.109119.

[7] O. Yadav, K. Passi, and C. K. Jain, "Using deep learning to classify x-ray images of potential tuberculosis patients," in *2018 IEEE International Conference on Bioinformatics and Biomedicine (BIBM)*, Dec. 2018, pp. 2368–2375, doi: 10.1109/bibm.2018.8621525.

[8] T. Rahman *et al.*, "Reliable tuberculosis detection using chest x-ray with deep learning, segmentation and visualization," *IEEE Access*, vol. 8, pp. 191586–191601, 2020, doi: 10.1109/access.2020.3031384.

[9] C. Dasanayaka and M. B. Dissanayake, "Deep learning methods for screening pulmonary tuberculosis using chest x-rays," *Computer Methods in Biomechanics and Biomedical Engineering: Imaging & Visualization*, vol. 9, no. 1, pp. 39–49, Aug. 2020, doi: 10.1080/21681163.2020.1808532.
[10] K. Munadi, K. Muchtar, N. Maulina, and B. Pradhan, "Image enhancement for tuberculosis detection using deep learning," *IEEE Access*, vol. 8, pp. 217897–217907, 2020, doi: 10.1109/access.2020.3041867.
[11] M. T. Islam, M. A. Aowal, A. T. Minhaz, and K. Ashraf, "Abnormality detection and localization in chest x-rays using deep convolutional neural networks," *arXiv preprint arXiv:1705.09850*, 2017.
[12] M. Ahsan, R. Gomes, and A. Denton, "Application of a convolutional neural network using transfer learning for tuberculosis detection," in *2019 IEEE International Conference on Electro Information Technology (EIT)*, May 2019, pp. 427–433, doi: 10.1109/eit.2019.8833768.
[13] U. K. Lopes and J. F. Valiati, "Pre-trained convolutional neural networks as feature extractors for tuberculosis detection," *Computers in Biology and Medicine*, vol. 89, pp. 135–143, Oct. 2017, doi: 10.1016/j.compbiomed.2017.08.001.
[14] M. B. Mizan, M. A. M. Hasan, and S. R. Hassan, "A comparative study of tuberculosis detection using deep convolutional neural network," in *2020 2nd International Conference on Advanced Information and Communication Technology (ICAICT)*, Nov. 2020, pp. 157–161, doi: 10.1109/icaict51780.2020.9333464.
[15] K. Cao, J. Zhang, M. Huang, and T. Deng, "X-ray classification of tuberculosis based on convolutional networks," in *2021 IEEE International Conference on Artificial Intelligence and Industrial Design (AIID)*, May 2021, pp. 125–129, doi: 10.1109/aiid51893.2021.9456476.
[16] E. Showkatian, M. Salehi, H. Ghaffari, R. Reiazi, and N. Sadighi, "Deep learning-based automatic detection of tuberculosis disease in chest X-ray images," *Polish Journal of Radiology*, vol. 87, pp. 118–124, Feb. 2022, doi: 10.5114/pjr.2022.113435.
[17] A. Shati, A. Datta, A. Mansoor, and G. M. Hassan, "ETDHDNet: An advanced DenseNet-based extended texture descriptor for efficient tuberculosis prediction in CXR images," *Intelligence-Based Medicine*, vol. 12, p. 100269, 2025, doi: 10.1016/j.ibmed.2025.100269.
[18] M. Salvi, U. R. Acharya, F. Molinari, K. M. Meiburger, "The impact of pre- and post-image processing techniques on deep learning frameworks: A comprehensive review for digital pathology image analysis," *Computers in Biology and Medicine*, vol. 128, 2021, doi: 10.1016/j.compbiomed.2020.104129.
[19] S. Park, J. Kim, S. Wang, and J. Kim, "Effectiveness of image augmentation techniques on non-protective personal equipment detection using YOLOv8," *Applied Sciences*, vol. 15, no. 5, p. 2631, 2025, doi: 10.3390/app15052631.
[20] R. M. Dyke and K. Hormann, "Histogram equalization using a selective filter," *Visual Computer*, vol. 39, pp. 6221–6235. 2023, doi: 10.1007/s00371-022-02723-8.
[21] W. Su *et al.*, "An XGBoost-Based knowledge tracing model," *International Journal of Computational Intelligence Systems*, vol. 16, no. 13, 2023, doi: 10.1007/s44196-023-00192-y.
[22] Index of public/Tuberculosis-Chest-X-ray-Datasets, "National library of medicine," 2024-08-28. [Online]. Available:https://data.lhncbc.nlm.nih.gov/public/Tuberculosis-Chest-X-ray-Datasets/index.html
[23] NIAID TB Portals Program, "National Institute of allergy and infectious diseases," July, 2025. [Online]. Available:https://tbportals.niaid.nih.gov/
[24] Tuberculosis (TB) Chest X-ray Database, kaggle, 2020. [Online]. Available: https://www.kaggle.com/datasets/tawsifurrahman/tuberculosis-tb-chest-xray-dataset
[25] Global Tuberculosis Report 2025, WHO, 2025-11-12.[Online]. Available: https://www.who.int/publications/i/item/9789240116924

BIOGRAPHIES OF AUTHORS

Abdul Karim Siddiqui received his first degree from SHUATS, Allahabad-India, in Computer Application, in 2007 and the Masters from AKTU, Lucknow-India in Computer Application, in 2011. He is enrolled as regular Ph.D. program from LPU- Punjab, India. His main research interests focus on deep learning, data mining, programming and image processing and MPL. He may be contacted at email: abdul.momentum@hotmail.com.

Dr Vijay Kumar Garg keeps a doctorate degree in Computer Science. He is professor in School of Computer Science and Engineering – LPU- Punjab, India. His specialized area is DL, ML, object-oriented programming, human computer interaction and image processing. He has published more than 40 research papers and tens of book chapters. Currently, he is program Coordinator in the department of Science and Technology in LPU-Phagwara. He can be contacted at email: vijay.garg@lpu.co.in.